文章编号:1007 – 6492(2000)04 – 0007 – 05

Finite Element Analysis of the Characteristics of the Thrust Floating Ring in Hybrid Sliding Cylindric Bearing

HUA Shao – jie, GUO Hong, XIA Bo – qian,
ZHANG Shao – lin, QI Jian – zhong, CEN Shao – qi

(College of Mechanical & Electronic Engineering, Zhengzhou University of Technology, Zhengzhou 450002, China)

Abstract: This paper has analysed the characteristics of the thrust floating ring in hybrid sliding cylindric bearing by finite element method. It also has presented balance conditions of the thrust floating ring and design criteria. The static and dynamic properties and stability parameters of the bearing have been obtaind on the basis of solution to the distribution of pressure fields of the inner and outer films and the dynamic Reynolds equations.

Key words: hybrid sliding bearing; radial floating ring; thrust floating ring; inner and outer oil films

CLC number: TH 117 **Document code**: A

Introduction

It is the key problem not to be ignored that the temperature rises higher as a result of power loss by friction in hybrid sliding bearings of high speed and high precision rotary system. Especially, when the axial load is heavy with high rotary speed, the functions of hybrid bearing will drop down obviously due to the rapid rise of centrifugal force and power loss in the combined structure of ordinary radial bearing and thrust bearing.

To control the temperature rise under high speed condition, we designed the radial floating ring and the thrust floating ring as an integral body. In this paper, the characteristics of the thrust floating ring in hybrid bearing have been analyzed by finite element method. The balance conditions of the thrust floating ring and the design criteria are also presented. The stability parameters of the bearing have been obtaind on the basis of solutions to the distribution of the pressure fields of inner and outer films and the dynamic Reynolds equations. The bearing's advantages of low power loss, low temperature rise and the use value that it possess have been proved by theoretical computation and experimental data.

1 The Bearing Structure and Principle[1,2]

This kind of bearing has a floating ring between bearing metal and shaft. The ring is designed to be integral body with radial and thrust rings as Fig.1. The inner oil film takes shape between the inner surface of ring and the shaft, the outer oil film takes shape between the outer surface of ring and the bearing metal. The ring is rotated by shearing stress in inner film when the shaft revolves with angular velocity Ω_1. Evidently, the angular velocity Ω_2 of the ring is the result of common acting on the ring by inner and outer films. The ratio, $\bar{\Omega} = \Omega_2/\Omega_1$, is the volume determined by the floating forces and moment of turning friction force loaded on the ring in films. The bearing with floating ring can work stably under certain ratio of ring turn velocity only when the forces suffered by ring are situated in balance. The presence of the relative velocity $(\Omega_1 - \Omega_2)$ must reduce the power loss due to friction and increase the stability in high speed bearing. Because of the uncompressibility and the vibration absorbability of oil films, the outer film let the whole body of the bearing be in elastic condition at the same time. Also, through the proper control of film thickness, the turnning precision that we need can be obtained. The thrust pockets

Received date: 2000 – 04 – 12; **revision received date**: 2000 – 06 – 11

Foundation item: Sponsored by the National Natural Science Foundation of China(59875080)

Biography: HUA Shao – jie(1944 –), male, born in Tianjin, professor of Zhengzhou University of Technology, research interests: lubrication theory & bearing technology.

are on the two sides of the thrust ring as Fig.2. The eight – pocket form is adopted for inner and outer films. The clearance between shaft and pockets on the inner surface of the ring has the function of second throttle as an inside flat capillary and avoids the blocking up in throttles effectively.

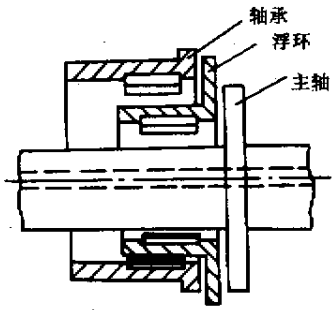

Fig.1 The bearing structure

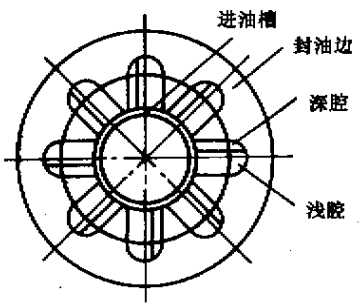

Fig.2 The thrust ring

2 Theoretical Computation and Analyses

2.1 The mathematics model[3,4]

In operating process, the movement of oil particles consumes energy constantly owing to its viscosity. The temperature field that is unevenly distributed is caused by oil films. The oil viscosity will decrease along with the temperature ascension, so the uneven temperature field must cause the uneven viscosity field.

We suppose that the all quantity of heat is transferred to outside by oil flowage. The dimensionless forms of Reynolds equation and Energy equation for inner and outer films of the thrust ring are as follows:

Reynolds equation:

$$\frac{\partial}{\partial\lambda_i}\left(\lambda_i H_i^3\frac{\partial\bar{P}_i}{\partial\lambda_i}\right)+\frac{1}{\lambda_i}\cdot\frac{\partial}{\partial\theta_i}\left(H_i^3\frac{\partial\bar{P}_i}{\partial\theta_i}\right)=6\mathrm{BNUM}_i\left(\frac{R_i}{L_i}\right)^2\frac{\partial H_i}{\partial\theta_i}\lambda_i, \tag{1}$$

$$\bar{P}=P/P_s,$$

Here P_s is pump pressure.

$$\mathrm{BNUM}_1=\frac{\mu(\Omega_1-\Omega_2)L_1^2}{P_sC_1^2},$$

$$\mathrm{BNUM}_2=\frac{\mu\Omega_2L_2^2}{P_sC_2^2},$$

boundary conditions:

$$\begin{cases}\bar{P}_i=1.0 & (i\in\Gamma_1);\\ \bar{P}_i=0.0 & (i\in\Gamma_2),\end{cases}$$

inner film: $i=1$, outer film: $i=2$.

Energy equation:

$$\left[\left(1-\frac{H_i^2}{6\mathrm{BNUM}_i}\frac{\partial\bar{P}_i}{\partial\theta_i}\right)\frac{\partial\bar{T}_i}{\partial\theta_i}-\frac{H_i^2}{6\mathrm{BNUM}_i}\left(\frac{R_i}{L_i}\right)^2\frac{\partial\bar{P}_i}{\partial\lambda_i}\frac{\partial\bar{T}_i}{\partial\lambda_i}\right]=\mathrm{TNUM}_i\cdot\left\{\frac{1}{H_i^2}+\frac{H_i^2}{12\mathrm{BNUM}_i}\left[\left(\frac{\partial\bar{P}_i}{\partial\theta_i}\right)^2+\left(\frac{R_i}{L_i}\right)^2\left(\frac{\partial\bar{P}_i}{\partial\lambda_i}\right)^2\right]\right\}, \tag{2}$$

$$\mathrm{TNUM}_i=\mathrm{BNUM}_i\frac{2P_s}{J\rho C_v}.$$

boundary conditions: $\bar{T}_i=1.0\quad(i\in\Gamma_1,\Gamma_2)$.

Dimensionless film thickness:

$$H_i=\begin{cases}1.0+Hs_i, & Hs_i\text{: depth of deep pockets};\\ 1.0+Hq_i, & Hq_i\text{: depth of shallow pockets};\\ 1.0.\end{cases}$$

Dimensionless viscosity – temperature equation:

$$\bar{M}_i=\alpha\cdot e^{-\beta\bar{T}_i},\ \bar{M}=\mu/\mu_0, \tag{3}$$

Here μ_0 is the viscosity at T_0.

Suppose the viscosity changes only with temperature and is not in close relationship with oil pressure. The definitions of other parameters that are not defined are as the same as normal standards.

2.2 The finite element analyses of basic equations[5]

The two – dimensional, eight – node and equal parameter units are adopted for the mesh divisions. And the form functions N_i have been selected as weighting functions. The Reynolds equation and the Energy equation can be separated into relevant differential equations by using the Галер Кун weight remainder method. The pressure field, the temperature field and the static – dynamic characteristics of the bearing can be obtained by deducing the equations.

2.2.1 The selection of form function

With two – dimensional, eight – node and equal parameter units, the form function N_i can be as follows:

$$N_0=\frac{1}{4}(1-\xi)(1-\eta)(-\xi-\eta-1);$$

$$N_1 = \frac{1}{4}(1-\xi)(1+\eta)(-\xi+\eta-1)\ ;$$

$$N_2 = \frac{1}{4}(1+\xi)(1+\eta)(\xi+\eta-1)\ ;$$

$$N_3 = \frac{1}{4}(1+\xi)(1-\eta)(\xi-\eta-1)\ ;$$

$$N_4 = \frac{1}{2}(1-\eta^2)(1-\xi)\ ;$$

$$N_5 = \frac{1}{2}(1-\xi^2)(1-\eta)\ ;$$

$$N_6 = \frac{1}{2}(1-\eta^2)(1+\xi)\ ;$$

$$N_7 = \frac{1}{2}(1-\xi^2)(1-\eta)\ .$$

2.2.2　The finite element equations of Reynolds inner film:

$$[K_1]\{P_1\} = \{F_1\}\ ; \qquad (4)$$

$$K_{1ij} = \iint_{\Omega^R}\left(\lambda_1 H_1^3 \frac{\partial N_i}{\partial \lambda_1}\frac{\partial N_j}{\partial \lambda_1} + \frac{H_1^3}{\lambda_1}\frac{\partial N_i}{\partial \theta_1}\frac{\partial N_j}{\partial \theta_1}\right)\mathrm{d}\Omega\ ;$$

$$F_{1ij} = \iint_{\Omega^R} 6\cdot\lambda_1\cdot H_1\cdot \mathrm{BNUM}_1\left(\frac{R_{21}}{L_1}\right)^2\frac{\partial N_i}{\partial \theta_1}\mathrm{d}\Omega\ ,$$

$i,j = 0,1,\cdots,7$,

outer film:

$$[K_2]\{P_2\} = \{F_2\}\ ; \qquad (5)$$

$$K_{2ij} = \iint_{\Omega^R}\left(\lambda_2 H_2^3 \frac{\partial N_i}{\partial \lambda_2}\frac{\partial N_j}{\partial \lambda_2} + \frac{H_2^3}{\lambda_2}\frac{\partial N_i}{\partial \theta_2}\frac{\partial N_j}{\partial \theta_2}\right)\mathrm{d}\Omega\ ;$$

$$F_{2ij} = \iint_{\Omega^R} 6\cdot\lambda_2\cdot H_2\cdot \mathrm{BNUM}_2\left(\frac{R_{22}}{L_2}\right)^2\frac{\partial N_i}{\partial \theta_2}\mathrm{d}\Omega\ ,$$

$i,j = 0,1,\cdots,7$.

2.2.3　The finite element equations of Energy

With the same separation method, we can get the linear algebraic equations of Energy:

$$[K]\{T\} = \{F\}\ , \qquad (6)$$

$$K_{ij} = \iint_{\Omega}\left[N_i\left(1-\frac{H^2}{6\mathrm{BNUM}}\frac{\partial P}{\partial \theta}\right)\frac{\partial N_i}{\partial \theta} - \frac{N_i H^2}{6\mathrm{BNUM}}\left(\frac{R^2}{L}\right)^2\frac{\partial P}{\partial \lambda}\frac{\partial N_j}{\partial \lambda}\right]\mathrm{d}\Omega\ ;$$

$$F_{ij} = \iint_{\Omega}\left\{N_i\cdot\mathrm{TNUM}\frac{1}{H^2} + \frac{N_i H^2 \mathrm{TNUM}}{12\mathrm{BNUM}^2}\left[\left(\frac{\partial \bar{P}}{\partial \theta}\right)^2 + \left(\frac{R_2}{L}\right)^2\left(\frac{\partial P}{\partial \lambda}\right)^2\right]\right\}\mathrm{d}\Omega\ ,\quad i,j = 0,1,\cdots,7\ .$$

In the deduing of equations with finite element method, the initial temperature field is granted at first, and then the pressure field is deduced from Reynolds equations, later on to deduce the temperature field with Energy equations based on every node pressure. In the end, the viscosity of all nodes is obtained using the $T \sim \mu$ equation. The pressure field will be computed again with the new viscosity. It is a alternative process repeatedly until getting the balance of the forces in inner and outer films. The relative convergence criteria of the alternative process is showed as follows:

$$\frac{|\bar{P}_{i,j}^{(k+1)} - P_{i,j}^{(k)}|}{|\bar{P}_{i,j}^{(k+1)}|} \leqslant 10^{-3}, \qquad (7)$$

The relative convergence precision of T field is controlled up to 4‰.

2.3　The analyses for results of computation[6]

Because of the turning conditions that are the high speed and high axial load, the design for the thrust part of the bearing with whole body ring is the crux evidently. The balance of the forces which acts on the ring through inner and outer films must be solved at first. For this reason, the static pressure balance will be gotten by regulations of pocket depthes, oil seal widthes and bearing clearance. Therefore, we can gain the initial design parameters that will be adjusted in dynamic pressure computation later on and sent back to static pressure computation again until satisfaction. The initial design parameters are as following:

pump pressure $P_s = 0.98$ MPa;
viscosity $\mu = 4.475\times10^{-3}$ Pa·s;
shaft's revol. $n = 38000$ r/min;
ring's rate $\bar{\Omega} = 0.3$;
number of pockets: 8;
thickness of films: 0.04 mm;
depth of deep pocket: 0.08 mm;
depth of shallow pocket: 0.02 mm.

2.3.1　The pressure field

The pressure fields of single pocket in inner and outer films have been obtained under variant shaft's revolutions and eccentric rates using the computation program and CG as Fig.3, Fig.4.

Based on table 1, the static effect is the main loading capacity when the speed becomes lower. With the speed rising, the pressure crest value increases sharply, which is the dynamic effect. It proved that the bearing has the better properties under lower and higher shaft's revolutions.

2.3.2　The power loss by friction

The eccentric rate will become larger with the load increasing. The relationship of power loss and eccentric

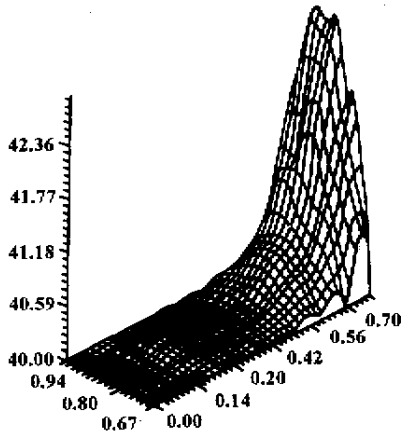

Fig.3 The pressure field of inner film, $\varepsilon = 0.7$, $\Omega = 38000$

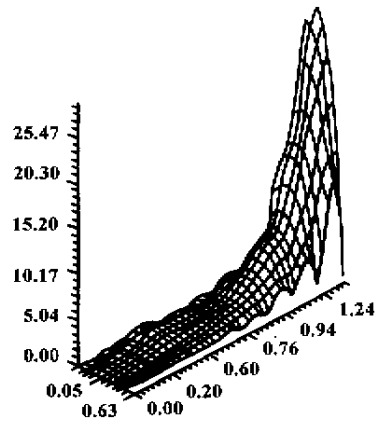

Fig.4 The pressure field of outer film, $\varepsilon = 0.7$, $\Omega = 38000$

rate is showed by Fig.5, Fig.6. The change regularities of curves are the same as load capacity 's. The power loss by friction is derived from the resistance of shear flow and pressure flow. And the former is direct ratio to the speed. Therefore the power loss increases with shaft 's revolution.

Table 1 The static properties in start process

shaft 's revol./(r/min)	film	clearance/mm	load capacity/N	power loss/kW	flow/(L/min)	ring 's rate
20000	inner	0.03730	2413	0.935	3.255	0.320
	outer	0.04270	2407	0.196	0.476	
25000	inner	0.03740	2471	1.295	5.013	0.330
	outer	0.04260	2508	0.337	0.539	
30000	inner	0.03750	2495	1.877	3.937	0.315
	outer	0.04250	2536	0.435	0.648	
38000	inner	0.0400	2743	2.852	3.638	0.30
	outer	0.0400	2782	0.655	0.776	

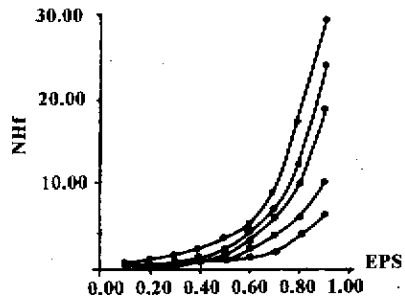

Fig.5 The power loss by friction of inner film

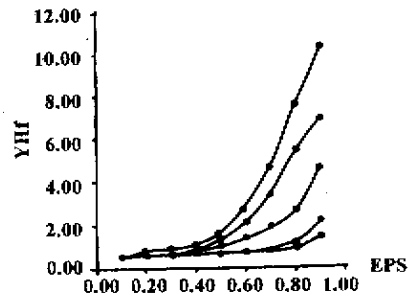

Fig.6 The power loss by friction of outer film

3 The Research of Experiment

Through the measurement for the static and dynamic characteristics of the hybrid bearing with ring and the comparison with the pure dynamic bearing, as shown in table 2, we know that the axial load capacity is 2782 N which meets the need; the power loss is redued by 39.5%; the turning rate of stability loss is 125685 r/min which is much higher than shaft 's and all the above properties prove the shaft runs stably.

Table 2 The comparison of characteristics

bearing	load capacity/N	power loss/kW	$\bar{\Omega}$	rate of stability loss/(r/min)
hybrid bearing(thrust part), inner	2743	2.852	0.300	125685
hybrid bearing (thrust part), outer	2782	0.655	0.300	125685
dynamic bearing	1000	4.716	–	3252789

4 Conclusions

(1) The hybrid bearing with integral ring has the advantages of simple structure, low power loss, easy temperature control compared with ordinary bearings.

(2) Through the computations of pressure field, power loss, static – dynamic properties and the critial turning rate, it is proved that this kind bearing has more stable capacity under high speed.

(3) The feasibility and the use value of the balance condition and the design criteria for the ring bearing are proved by the compute results and the experimental data.

References:

[1] ZHANG Zhi – ming. The Hydrodynamic Lubrication Theory of Sliding Bearing[M]. Beijing: Higher Education Publishing House, 1987. 108 – 119.

[2] OSCAR Pinkus, BENO Sternlicht. Theory of Hydrodynamic Lubrication[M]. England: McGraw – hill Book Company, 1961. 227 – 325.

[3] CAMERON A. Basic lubrication Theory[M]. England: Longman Book Company, 1976. 57 – 66.

[4] XU Shang – xian. The Design of Hybrid Bearing[M]. Nanjing: Southeast University Publishing House, 1987. 250 – 319.

[5] XIA Heng – qing. The Principle and Design of Hydrostatic Bearing[R]. Zhengzhou: Zhengzhou Institute of Technology, 1984. 31 – 60.

[6] 梁　辉, 郭　红, 张少林, 等. 动静压浮环电主轴基本理论研究[J]. 郑州工业大学学报, 1999, 20(2): 64 – 66.

圆柱浮环液体动静压轴承止推环性能的有限元分析

华绍杰, 郭　红, 夏伯乾, 张少林, 祁建中, 岑少起

(郑州工业大学机械与电子工程学院, 河南 郑州 450002)

摘　要: 对圆柱浮环液体动静压轴承止推环的静、动态特性进行了有限元分析, 提出了保证浮环正常工作的平衡条件, 并据此给出了浮环轴承的设计准则. 在有限元分析中求解了该轴承内、外膜压力场, 分析了动态雷诺方程. 在求得浮环静压、动压平衡的基础上, 得到了该轴承的静、动态特性及稳定性参数.

关键词: 动静压滑动轴承; 径向浮环; 止推浮环; 内外层油膜